Improving the quantification of Brownian motion

Marco A. Catipovic, Paul M. Tyler, Josef G. Trapani, and Ashley R. Carter

Citation: Am. J. Phys. **81**, 485 (2013); doi: 10.1119/1.4803529
View online: http://dx.doi.org/10.1119/1.4803529
View Table of Contents: http://ajp.aapt.org/resource/1/AJPIAS/v81/i7
Published by the American Association of Physics Teachers

Improving the quantification of Brownian motion

Marco A. Catipovic, Paul M. Tyler, Josef G. Trapani, and Ashley R. Carter[a)]
Amherst College, Amherst, Massachusetts 01002

(Received 29 November 2012; accepted 15 April 2013)

Brownian motion experiments have become a staple of the undergraduate advanced laboratory, yet quantification of these experiments is difficult, typically producing errors of 10%–15% or more. Here, we discuss the individual sources of error in the experiment: sampling error, uncertainty in the diffusion coefficient, tracking error, vibration, and microscope drift. We model each source of error using theoretical and computational methods and compare the model to our experimental data. Finally, we describe various ways to reduce each source of error to less than 1%, improving the quantification of Brownian motion. © *2013 American Association of Physics Teachers.*
[http://dx.doi.org/10.1119/1.4803529]

I. INTRODUCTION

A classic experiment in the undergraduate advanced laboratory is to measure Brownian motion by observing microscopic particles in solution.[1–13] The particles, contrary to our everyday experience, do not fall directly to the bottom of the sample chamber according to their density, but are instead bombarded by solution molecules. The particles may move left, then right, stop, descend, move backward, and stop again, in a series of displacements collectively named Brownian motion after the botanist Robert Brown, who described this movement for pollen amyoblasts in 1828.[14]

The popularity of this experiment is due to both the simplicity of the apparatus and the historical importance of the data in proving the atomic nature of matter. At the turn of the 20th century, prominent chemist and Nobelist Wilhelm Ostwald posited that matter was a manifestation of energy, rejecting the widespread atomistic view. To address this debate, Einstein, in a landmark paper in 1905, theorized that the random movements of a particle undergoing Brownian motion could be completely explained by molecular-kinetic theory.[15] Because Einstein's theory depended on the atomic nature of matter, the subsequent measurement of Brownian motion by Jean Baptiste Perrin[16] was pivotal in proving the atomistic view and earned Perrin the 1926 Nobel Prize. Today, this historically significant experiment is used to visualize a random walk and can also be used to measure a number of interesting parameters: the viscosity of the solution,[11] the Boltzmann constant,[5,8] or Avogadro's number,[10] to name a few.

Unfortunately, the data obtained in these Brownian-motion experiments are somewhat disappointing for students, as measurements can easily be off by 10%–15% or more.[1,5,8,11,12] This large discrepancy between the measured and nominal values generates a series of questions: What are the dominant sources of error in the experiment? How much error should we expect for a given source? And, how can we reduce these sources of error?

Our goal is to address these questions and improve the quantification of Brownian motion experiments. In Sec. II, we discuss a simple implementation of the experiment that produces measured results with errors of 15%–30%. In Sec. III, we theoretically and computationally model a number of possible noise sources: sampling error, uncertainty in the diffusion coefficient, tracking error, vibration, and microscope drift. We compare our computational model of these noise sources to our experimental data, highlighting the largest sources of noise in the experiment and providing a framework for calculating an expected noise value. Finally, in Sec. IV, we discuss ways to minimize these noise sources and produce results that are within 1% of the nominal value. In this way, we hope to provide a method for both diagnosing and reducing noise in Brownian motion measurements.

II. EXPERIMENTAL MATERIALS AND METHODS

In our implementation of the experiment [Fig. 1(a)], micron-sized polystyrene beads (Invitrogen, Fluospheres, Lot # 1154194, radius = 0.550 μm ± 3.2%) are diluted in water and imaged using a microscope (Leitz, Labovert FS, 100× oil-immersion objective, numerical aperture = 1.3). Concentrations at 0.09 pM (0.004% w/v) produce 10 or so beads in the field of view. Sample chambers (30 × 10 × 0.3 mm) are made by placing four pieces of double-sided tape between a cover slip and a microscope slide. Chambers are sealed with epoxy to prevent evaporation and fluid flow. Beads typically spend ∼30 s in the field of view.

To quantify Brownian motion, a megapixel camera (Thorlabs DCC1545M, 5-ms exposure, 100-ms acquisition time) records the movement and a software tracking program (IMAGEJ, plugin MTRACK2[17]) post-processes the images and extracts the particle positions to form tracks [Figs. 1(b)–1(d)]. We analyze two videos to produce $N = 15$ tracks that each contain 100 frames at 10 Hz. Collection of the data and processing of the tracks takes about an hour, perfect for a laboratory course.

Theoretically, the motion in x and y follows a random walk such that the two-dimensional mean displacement $\langle \Delta r \rangle$ is zero and the mean-squared-displacement (MSD) $\langle \Delta r^2 \rangle$ is given by

$$\langle \Delta r^2 \rangle = \langle \Delta x^2 \rangle + \langle \Delta y^2 \rangle = 4Dt. \quad (1)$$

Here, $\langle \Delta x^2 \rangle$ and $\langle \Delta y^2 \rangle$ are the one dimensional MSDs, D is the diffusion coefficient, and t is the time between data points. (On the time scale of our experiment, with a 100-ms acquisition time, the average, two-dimensional root-mean-squared (rms) displacement of 400 nm per frame will be made up of many smaller steps. A back-of-the-envelope calculation reveals that the mean-free-path of a 1-μm-diameter bead is about 0.3 nm,[18] three orders of magnitude smaller. To visualize this motion, the online supplement to this article[19,32] includes a simulation in the IGOR programming language that allows students to vary the parameters of an idealized two-dimensional random walk of the bead.)

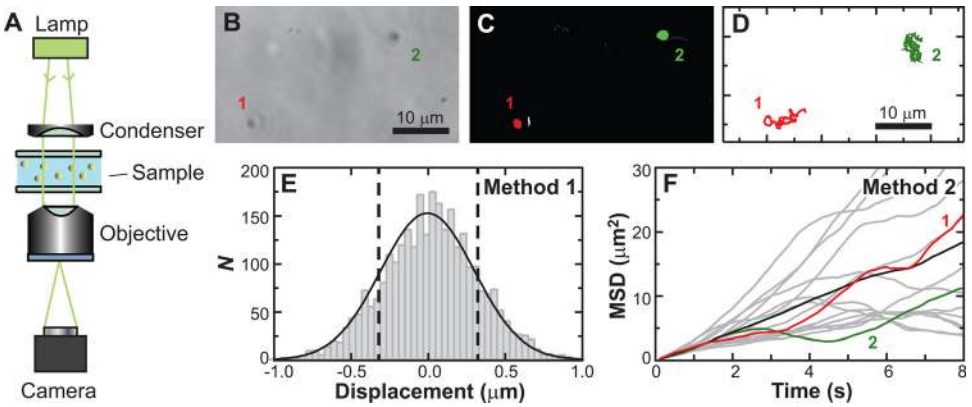

Fig. 1. (Color online) A simple implementation of the Brownian-motion experiment produces data with 15%–30% error. (a) Cartoon showing a bright field microscope that images micron-sized polystyrene beads undergoing Brownian motion in water. (b) Image taken at 100× magnification; beads (labeled 1 and 2) are just below the focal plane and appear black. (c) Post-processing produces a binary image. (d) The position of each particle in x and y is extracted for each frame and placed into a track. (e) In Method 1, the diffusion coefficient is found by making a histogram of the displacements in both x and y (gray) and fitting a Gaussian curve (black line) to the data; the standard deviation (dashed black lines) is used to calculate a diffusion coefficient of 0.512 μm^2/s, a difference of 15.1% from the nominal value. (f) In Method 2, the mean squared displacement (MSD) of each particle (gray) as a function of time is averaged together (black) and the slope of the line is used to find a diffusion coefficient of 0.575 μm^2/s, a difference of 29.2%. Labeled MSD traces correspond to the particles shown in B through D.

This random walk, given by Eq. (1), varies with the diffusion coefficient and time. The rms displacement increases in proportion to $\sqrt{t}$, allowing the bead to rapidly sample the surrounding area on short timescales, yet requiring long timescales to move greater distances. Brownian motion also increases with increasing temperature T or decreasing bead radius a, as both of these variables are wrapped up in the diffusion coefficient

$$D = \frac{k_B T}{6\pi\eta a} = \frac{R}{N_A}\frac{T}{6\pi\eta a}. \tag{2}$$

Here, k_B is the Boltzmann constant, η is the viscosity of the solution, R is the ideal gas constant, and N_A is Avogadro's number. In a typical undergraduate laboratory students may be asked to record data for ~10 beads and to measure the diffusion coefficient. Subsequent calculations may require the students to solve for the Boltzmann constant, Avogadro's number, the radius of the bead, or the temperature of the solution.

In our implementation of the experiment, we measure the diffusion coefficient using the two most common methods. In Method 1, we fit a Gaussian to the displacement histogram [Fig. 1(e)], a histogram that bins all the independent, one-dimensional displacements, both Δx and Δy, together. The variance from the Gaussian fit is equivalent to the one-dimensional MSD $\langle \Delta x^2 \rangle$ if the mean displacement $\langle \Delta x \rangle$ is zero

$$\mathrm{Var}(\Delta x) = \langle \Delta x^2 \rangle - \langle \Delta x \rangle^2. \tag{3}$$

Because our data in $\langle \Delta x \rangle$ and $\langle \Delta y \rangle$ have a zero mean displacement (6 ± 8 nm and 0 ± 8 nm, respectively), we can use the variance of the displacement histogram to calculate D through the one-dimensional random walk equation

$$\langle \Delta x^2 \rangle = 2Dt. \tag{4}$$

Using this method, we calculate $D = 0.512\ \mu$m^2/s, a difference of 15.1% from the nominal value of 0.445 μm^2/s. (Measurements were taken in water, $\eta = 0.89$ mPa-s, at a temperature of 24.9 °C).

In Method 2, we calculate the two-dimensional MSD at each time t using the equation

$$\langle \Delta r^2(t) \rangle = \frac{\sum_{i=1}^{N_i} [(x(t_i + t) - x(t_i))^2 + (y(t_i + t) - y(t_i))^2]}{N_i}, \tag{5}$$

where time t_i refers to the time for the ith image in the track and N_i is the number of images to compute the average over. For example, if we would like to compute the MSD of the $t = 3$ s time point for a track at 10 Hz, we would find the squared displacement between images 1 and 31, images 2 and 32, images 3 and 33, and so on. The average of these squared displacements would be the MSD at $t = 3$ s. After the MSD for each track is calculated we create an ensemble MSD by averaging all of the individual track MSDs [Fig. 1(f)]. The diffusion coefficient is determined from the slope of the ensemble MSD and Eq. (1) to be $D = 0.575\ \mu$m^2/s, a difference of 29.2% from the nominal value. Thus, both methods produce results with large errors (15%–30%). Our goal is to identify the source of this error through theoretical and computational modeling and to reduce it.

III. THEORETICAL AND COMPUTATIONAL MODELING OF ERROR

A. Sampling error

The noise floor in the experiment is set by sampling error. Sampling error is a statistical error created when only a subset of a population is sampled. The sampling error in Brownian motion experiments varies with the method used to determine the diffusion coefficient.

In Method 1, we measure the variance of a normally distributed variable, Δx or Δy. The sampling error, $\sigma_{\mathrm{sampling}}$, in this case, will then be the standard deviation of the variance. The fractional sampling error is

$$(\textbf{Method 1}) \quad \text{fractional } \sigma_{\text{sampling}} = \sqrt{\frac{2}{N-1}}, \tag{6}$$

as discussed in Appendix E in Taylor's *An Introduction to Error Analysis*.[20] Here, N is the number of samples in the histogram and the familiar expression $N-1$ is used to counteract the underestimate of the fractional error when a subset of the population is sampled. Thus, we would expect the fractional σ_{sampling} in a measurement of D with 15 tracks (100 frames per track) to be 0.026 or 2.6% ($N=3000$ total displacements from the two independent dimensions, x and y).

In Method 2, we measure the MSD, which is the sum of the squares of two normally distributed values. As such, we would expect the MSD to follow a chi-squared distribution. Thus, the σ_{sampling} would be the standard deviation in the mean value of the distribution, which is just the familiar standard error. The fractional sampling error would be

$$(\textbf{Method 2}) \quad \text{fractional } \sigma_{\text{sampling}} = \frac{1}{\sqrt{N}}. \tag{7}$$

In this case, the fractional σ_{sampling} for 15 tracks would be 0.26 or 26%, indicating that Method 2 has a much larger sampling error (by an order of magnitude) than Method 1. In an undergraduate laboratory where data collection will be limited, using Method 1 instead of Method 2 will decrease the amount of sampling error substantially. However, if the goal of the laboratory is to try to measure the viscosity of a complex liquid that may have an elastic component,[21] then Method 2 should be used as it does not automatically depend on the linearity of the MSD with time. We will continue to discuss both methods, noting that each will have a large sampling error.

In addition, we find that a computational simulation of the experiment (see the MATLAB code in the online supplement[19]) reproduces the theoretical sampling error for both Method 1 and Method 2 [Figs. 2(a) and 2(b)]. The simulation is based on a common procedure for measuring sampling error[20] that we and others[22] have adapted for use in Brownian motion experiments. We first create a series of random steps in both x and y with the standard deviation for each step set by the one dimensional random walk equation (4). We then concatenate the steps into a track and measure the diffusion coefficient using the two methods. The simulation parameters mirror the experimental variables ($T=24.9\,^{\circ}\text{C}$, $\eta=0.892\,\text{mPa-s}$, $a=0.550\,\mu\text{m}$, track length $=100$ frames, data rate $=10\,\text{Hz}$). In Method 1, we simulate a particular number of tracks and find the diffusion coefficient by measuring the variance of the x and y displacement histogram. In Method 2, we calculate the average ensemble MSD for all of the tracks and use the slope to compute D. These procedures give us the diffusion coefficients for Method 1 and Method 2 for one data set. We repeat this procedure 100 times to create 100 data sets with the same number of tracks in each. We find that as the number of tracks in a data set increases, the sampling error for both methods decreases according to Eqs. (6) and (7). Overall, some data sets fall outside the standard deviation set by the sampling error, but most are within $2\sigma_{\text{sampling}}$ as expected.

Interestingly, the error in our initial measurement of D using Method 2 can be explained entirely by sampling error, but this is not the case for Method 1. The fractional sampling error for Method 2 has a theoretical value of 26% ($N=15$ tracks), close to the actual error of 29%. However, the experimental error for Method 1 is 15%, while the fractional sampling error for the measurement is only 2.6% ($N=3000$ displacements). To explain this large discrepancy for Method 1 we must turn to other sources of error.

B. Uncertainty in the diffusion coefficient

Measurement of the nominal diffusion coefficient will have an error due to the uncertainty in the bead radius and temperature. The uncertainty in the bead radius is due to the size variation in the polystyrene beads, which is a Gaussian distribution with a standard deviation given by the coefficient of variation. Typical values are 2%–10% depending on the company and the size of the bead (Spherotech, Lot # AD01, $a=0.693\,\mu\text{m}\pm7.8\%$; Invitrogen, Lot # 1154194, $a=0.550\,\mu\text{m}\pm3.2\%$). The other independent variable, temperature, could slowly vary over time at the level of $1^{\circ}\text{C}\,(0.3\%)$ due to changes in room temperature or fluctuations in illumination intensity. In addition, this temperature

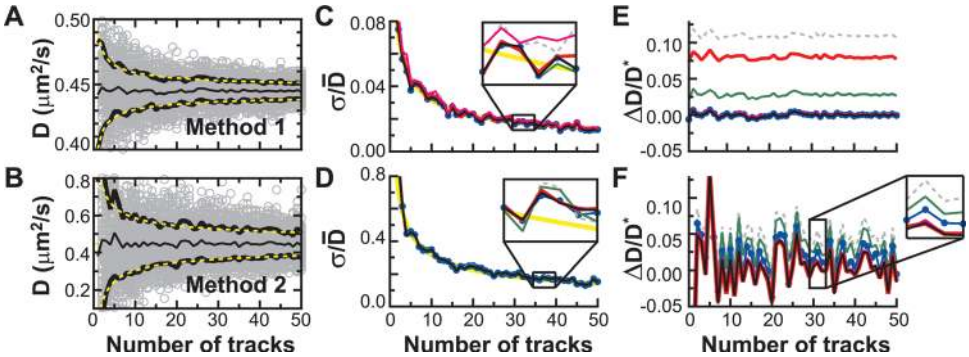

Fig. 2. Simulated data show that the largest sources of error in the experiment are sampling error, tracking error, and vibration. (a) and (b) The diffusion coefficients (D) from 5,000 simulated data sets are plotted (gray circles) as a function of the number of tracks in a data set for either Method 1 or Method 2. The standard deviation of the diffusion coefficient, σ (thick black line), follows the theoretical sampling error for each method (yellow dashed line). The mean value of the diffusion coefficient $\bar{D}$ (thin black line) tracks the nominal diffusion coefficient D^*, as expected. (c) through (f) Same data as in A and B (black line) except with the following added sources of error: uncertainty in the bead radius and temperature (magenta line); tracking error (thick red line); drift (blue filled circles); vibration (green line); and all of the above (gray dashed line). In (c) and (d) the fractional sample standard deviation $\sigma/\bar{D}$ remains virtually unchanged by the sources of error, and all of the traces are on top of the theoretical sampling error (yellow line). In (e) the fractional difference between the mean and nominal value of the diffusion coefficient $\Delta D/D^*$ shows that the simulated data with tracking error and vibration are above the noise floor set by sampling error in Method 1. In Method 2 (f), the sampling error causes large fluctuations in $\Delta D/D^*$.

variation will affect the macroscopic viscosity of water, which is a known function of temperature[23] (see the supplementary MATLAB file[19]). Given this function, a temperature uncertainty of 1°C would create a 2% uncertainty in the macroscopic viscosity. Thus, we have two independent sources of random error that contribute to the uncertainty in the nominal diffusion coefficient: variation in the bead radius and temperature fluctuations (for a discussion of systematic error see Appendix A).

If we assume that both sources of error are random and independent, then the central limit theorem would suggest that the uncertainty in D will be normally distributed and should decay with the number of samples in the data set.[24] To model this phenomenon, we simulate the same data as in Figs. 2(a) and 2(b), except instead of using the nominal value for the diffusion coefficient to generate the data we simulate random values from a Gaussian distribution for both the bead radius (standard deviation of 18 nm) and temperature (standard deviation of 1 °C). We use two metrics to measure the effect of this source of error. In the first metric we measure the precision of the measurement of D by plotting the fractional sample standard deviation of the data $\sigma/\bar{D}$ as a function of the number of tracks in the data set [Figs. 2(c) and 2(d)]. For Method 1, there is an increase of 0.2% in the fractional standard deviation, just above the noise floor set by the sampling error, but there is no change in Method 2. This means that the scatter in the data will be set by sampling error and will not be affected by the uncertainty in the diffusion coefficient. In the second metric accuracy is measured by subtracting the nominal value of the diffusion coefficient D^* from the simulated mean value $\bar{D}$ and dividing by the nominal value [Figs. 2(e) and 2(f)]. For both Method 1 and Method 2, $\bar{D}$ is not affected by the uncertainty in bead radius or temperature. These findings lead us to conclude that these uncertainties are small enough to be ignored in our experiment and should not factor into our calculation of error.

C. Tracking error

Brownian motion experiments also suffer from tracking error—the uncertainty in extracting the time and location of a bead in a series of images. Timing uncertainty is generally set by the image acquisition system and decreases if the exposure time (5 ms) is much less than the acquisition time (100 ms). In our system, timing uncertainty is 1–10 ms per frame at 10 Hz, which translates into a positional uncertainty of 1–15 nm. The uncertainty in locating the centroid of the bead is comparatively higher. In MTRACK2, bead location is found by using the IMAGEJ "Measure" command, which calculates the centroid by taking the mean value of all of the (x, y) pixel coordinates in the particle (a binary image of the bead). The error in finding this value is just the standard error of the mean, $\sigma/\sqrt{N}$. If the particle is a perfect circle, then the standard deviation of the centroid will be equal to half the radius of the circle, while the number of pixels N will be given by the area of the circle. The standard error then reduces to $\sigma/\sqrt{N} = (a/2)/\sqrt{\pi a^2} = 1/(2\sqrt{\pi})$, or 0.28 pixels (15 nm), and surprisingly does not depend on bead size. In practice, though, the error in tracking the centroid is closer to 1 pixel (60 nm) due to the irregular shape of the particle. Tracking error improves for beads within the focal plane as the higher contrast of the image enhances detection and increases the circularity of the particle. Here, we will take into account both timing and positional uncertainty to find the effect of tracking error on the measured diffusion coefficient.

To see the effect of tracking error, we simulate random values from a Gaussian distribution for both the uncertainty in the timing interval (standard deviation of 10 ms) and the particle position (standard deviation of 60 nm). Timing errors are converted into positional errors using the one-dimensional random-walk equation and added to the positional error in tracking the centroid, before calculating D using the two methods [Figs. 2(c)–2(f)]. In Method 1, we see an increase in the mean value of D by 8% due to tracking error. In contrast, the diffusion coefficient measured by Method 2 does not change at all. We might expect this to be the case as a tracking error of 60 nm would be relatively large compared to the displacement between frames (300 nm at 10 Hz) used in Method 1. In comparison, tracking error would be fairly small compared to the movement over the entire track (3 μm at 10 s) used in Method 2. We conclude from this simulation that we need to account for tracking error only when using Method 1.

D. Drift or vibrational noise

Typically, mechanical noise in the experiment can be broken down into two components: a drift between the sample and the objective that occurs over tens of seconds, and a faster vibration that causes jitter in the microscope. While our typical microscope drift is on order 1 nm/s (see Appendix B) due to settling of the focus knob, thermal expansion of the sample, or other low frequency mechanical noise, the most substantial source of drift in Brownian-motion experiments is fluid flow. Fluid flow (on orders of 0.01–10 μm/s in our samples) can occur because of evaporation, convection, the presence of bubbles, or the addition or removal of liquid from the sample. To prevent fluid flow and measure an average bead displacement of zero as in Fig. 1(e), samples should be sealed without bubbles and allowed to equilibrate for a few minutes. Equilibration over longer times (hours) should be avoided as this will cause settling of the beads.[25] The other source of mechanical noise, vibration, can cause movements at the level of 20–50 nm per frame at 10 Hz. Larger vibrations are also possible; for instance, touching the microscope or table may cause the sample to suddenly shift by several microns in one frame. Thus, noise sources may be problematic.

To model the effect of drift and vibrational noise on the measurement of the diffusion coefficient, we again use our simulated data from Figs. 2(a) and 2(b) and this time incorporate errors due to these noise sources. To simulate drift, we add a constant to the one dimensional displacement in y corresponding to 100 nm/s. Vibration is simulated by adding a random value to the x and y displacements from a Gaussian distribution with a standard deviation of 50 nm [Figs. 2(c)–2(f)]. We find that the simulated drift and vibrational noise have a large effect, increasing $\bar{D}$ by 3% in Method 1 (all due to vibrational noise) and 5% in Method 2 (3.5% from vibrational noise and 1.5% from drift) over the shown range. What is interesting is that even though the percent increase in $\bar{D}$ is higher in Method 2, the fluctuations due to sampling error are at about the same level. Therefore, sampling error is really the dominant source of error in Method 2, rendering all other sources of error negligible. However, if we further increase drift to 200 nm/s and vibrational noise to a standard deviation of 100 nm, then $\bar{D}$

increases by 11% in Method 1 and by 18% in Method 2. Even greater differences between the measured and nominal values are possible. For example, data can be off by factors of ten or more if there is fluid flow of 1 μm/s, highlighting just how important it is to reduce this source of error. Reduction of drift to less than 50 nm/s and vibration to within a standard deviation of 30 nm at 10 Hz produces negligible errors according to our computational model.

E. Multiple sources of error

In addition to modeling individual sources of error, we also modeled the total error in our system due to all of the different noise sources. Interestingly, drift, vibration, and tracking error all increase $\bar{D}$, indicating that the experiment will tend to overestimate the diffusion coefficient if these noise sources are present. We also note that the individual sources of error add together to give the total error for the data. Therefore, for Method 1, we would expect a measurement of D that is higher than the nominal value due to the errors associated with tracking error and vibrational noise. If we assume that there is an 11% error due to either tracking error or vibration, then we would expect Method 1 to produce a value within $2\sigma_{\text{sampling}}$ (6%) of 0.494 μm^2/s, which is higher than the nominal diffusion coefficient of 0.445 μm^2/s. Our experimental measurement of 0.512 μm^2/s agrees with this computational prediction. We would expect Method 2 to produce a result that is dominated by sampling error, which is the case.

Based on our computational model, we conclude that even though Method 1 produces a much more precise result, Method 2 might be more appropriate for the undergraduate laboratory. Method 1 requires calculation of the error from 3 to 4 different noise sources (sampling error, tracking error, vibration, and possibly uncertainty in bead radius and temperature), requiring a large amount of lab time to be spent on error analysis. In comparison, Method 2 is dominated by a large sampling error that is easily calculated by the students. The drawback with Method 2 is that it requires a large amount of data to measure the diffusion coefficient precisely. Alternatively, Method 1 can be implemented successfully in the undergraduate laboratory if the experiment is designed to minimize tracking error and vibrational noise.

IV. REDUCING ERROR

A. Experimental methods to reduce error

To improve the quantification of Brownian motion measurements, we employ several experimental techniques to reduce drift, vibration, and tracking error. First, we mount a microscope (Olympus BX-51WI, 40× water-immersion objective) onto a vibration-isolation table, reducing drift to $<$1 nm/s and vibration to $<$15 nm at 10 Hz. Further stabilization of the sample is possible in this configuration,[26] but was not implemented as this level of noise should be negligible according to our simulation. Second, we improve tracking error by (i) using a camera (Coolsnap EZ, Photometrics) with a higher quantum efficiency that improves image contrast, and by (ii) tracking beads with a program written in MATLAB.[27,28] Switching to this program allows for increased functionality in both post-processing of the images and in setting the tracking parameters. Correct implementation of this program limits tracking error to less than 20 nm.[27] With this improved experiment we measure a diffusion coefficient of $0.418 \pm 0.004\ \mu\text{m}^2/\text{s}$ (mean $\pm 2\sigma_{\text{sampling}}$) using Method 1 and $0.45 \pm 0.04\ \mu\text{m}^2/\text{s}$ using Method 2 (400 tracks, 100 frames per track, 10 Hz; see Fig. 3). Both measurements agree with the nominal value of 0.415 μm^2/s ($T = 22.4\,^\circ$C, $\eta = 0.946$ mPa-s, $a = 0.550\ \mu$m). Thus, by reducing vibrational noise, drift, and tracking error we are able to produce a measurement with Method 1 that is within 1% of the nominal value.

In addition, we find that image processing is improved if data is taken with an epifluorescence microscope (Olympus BX-51WI) that images fluorescent beads. Previous work has already discussed the use of inexpensive fluorescent microscopes in Brownian motion experiments, showing the feasibility of the technique in the undergraduate laboratory.[12] Here, we show that image contrast is much higher [Figs. 3(a) and 3(b)], eliminating the need to perform image background subtraction and reducing tracking error. In Figs. 3(c) and 3(d), we use this technique to track 200 beads (100 frames, 10 Hz) and measure a diffusion coefficient of $0.432 \pm 0.006\ \mu\text{m}^2/\text{s}$ using Method 1 and $0.45 \pm 0.06\ \mu\text{m}^2/\text{s}$ using Method 2. Both of these values agree with the nominal value of 0.430 μm^2/s

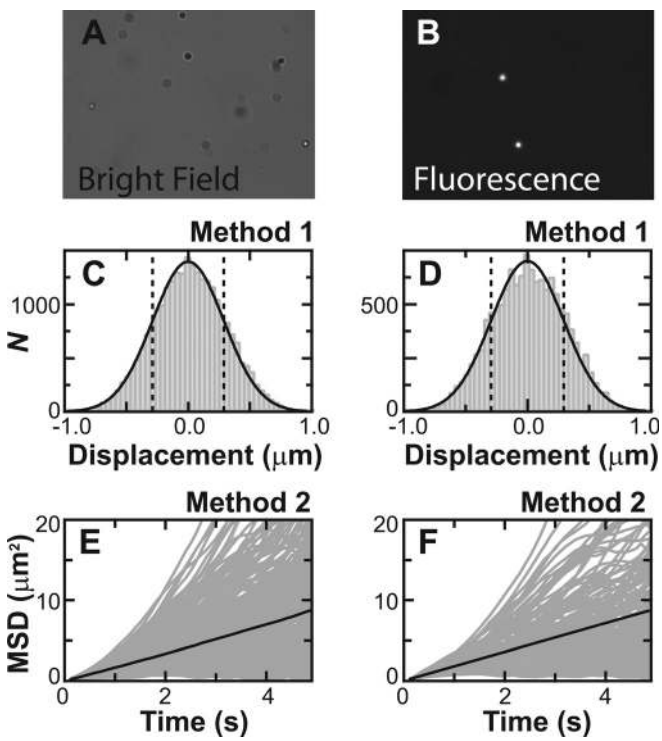

Fig. 3. Reduction of experimental noise produces measurements of D within 1%. Either bright field microscopy (a) or epifluorescence microscopy (b) can be used; however, fluorescence images have a higher contrast and do not require background subtraction. (c) and (d) Measurements of the diffusion coefficient D using Method 1 are found by fitting a Gaussian (black line) to a histogram of the tracked displacements (gray) to find the standard deviation (black dashed line). For bright field microscopy in (c), D is $0.418 \pm 0.004\ \mu\text{m}^2/\text{s}$ (mean $\pm 2\sigma_{\text{sampling}}$), within error of the nominal value of 0.415 μm^2/s. For epifluorescence microscopy in (d), D is $0.432 \pm 0.006\ \mu\text{m}^2/\text{s}$, also within error of the nominal value of 0.430 μm^2/s. (e) and (f) Measurements of D using Method 2 are found by fitting the slope of an averaged ensemble MSD (black) made up of individual MSDs for each track (gray). Here, D is found to be $0.45 \pm 0.04\ \mu\text{m}^2/\text{s}$ using bright field microscopy in (e), while fluorescence microscopy in (f) gives a D of $0.45 \pm 0.06\ \mu\text{m}^2/\text{s}$, both within error of the nominal values.

($T = 23.6\,^{\circ}\mathrm{C}$, $\eta = 0.919\,\mathrm{mPa} - \mathrm{s}$, $\mathrm{a} = 0.550\,\mu\mathrm{m}$). Thus, the diffusion coefficient measured using Method 1 is still within 1% of the nominal value, yet the data analysis is markedly faster.

B. Computational methods to reduce error

While we have shown that experimental improvements can greatly increase the accuracy of Brownian motion measurements, these improvements are both costly and time consuming. An alternative technique would be to use Method 2 and to combine the data from all of the different groups in the laboratory or to use a resampling technique[29] to increase the precision. However, even in this case, the sampling error in Method 2 can be prohibitively high; it requires 100 tracks to get a 10% sampling error. Ideally, then, we would like to use Method 1 because the sampling error is much lower. The problem is that we need to be able to reduce the other sources of error without resorting to expensive changes in the experimental apparatus. Here we seek to reduce the error in Method 1 though computational approaches.

Tracking error is the largest error in Method 1, and fortunately it can be reduced by improving the centroid-tracking algorithm. At first we decided to analyze our original data (Sec. II) with the MATLAB program[27] used previously. The greater functionality of this program allows us to easily optimize the input parameters to achieve accurate centroid-finding to within an estimated 20 nm. However, early on we noticed that the most important input parameter in the program is the one that sets the threshold for pixels to be included in the particle. The optimum setting allowed only beads that were in focus to be tracked, as the increased image contrast reduced the tracking error. This data suggested that it might be possible to reproduce the same results using IMAGEJ. Here we show that both MTRACK2 and the MATLAB program[27] produce similar tracks when processing the same images of a bead freely diffusing in solution or when processing images of a bead stuck to the cover slip (Fig. 4). The key is to set the threshold in IMAGEJ such that only beads that are in focus are tracked. If this simple change is made, we estimate that the tracking error is about the same in both cases. We then reanalyze our original data with the increased threshold value so that we only track beads within a small focal depth of a few hundred nanometers. To remove bias, the track length is decreased to 10 frames at 10 Hz as most beads spend >1 s in range. Amazingly, the new measured diffusion coefficient is within 1% of the nominal value at $0.450\,\mu\mathrm{m}^2/\mathrm{s}$ (180 tracks, $N = 10\,000$) as the mechanical noise is negligible (see Appendix B). This improvement does not require any additional equipment but does require some practice on the part of the user to select the appropriate threshold.

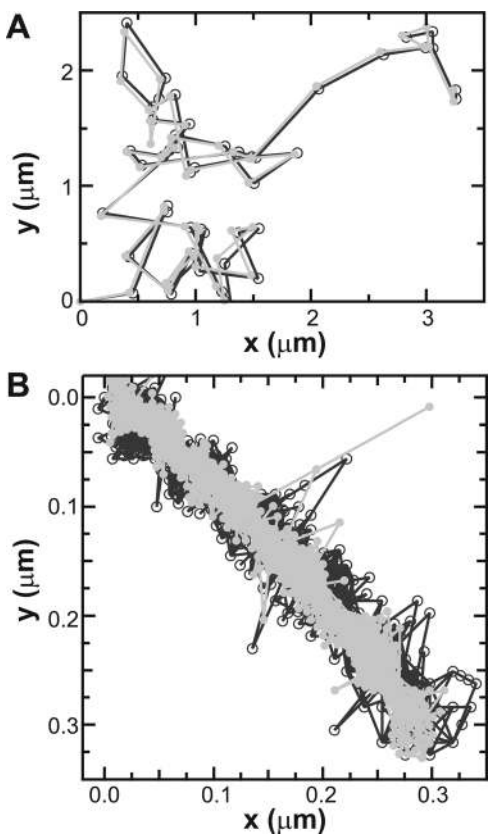

Fig. 4. Tracking with IMAGEJ or with a MATLAB program produces similar results. (a) We track a single bead undergoing Brownian motion in water with IMAGEJ MTRACK2 (gray closed circles), and a MATLAB tracking program with an improved centroid-finding algorithm[27] (black open circles). (b) We also track a bead stuck to the surface with both programs (colors same as in a).

V. CONCLUSIONS

Here, we have shown that the large ($\sim$15%) errors present in Brownian motion experiments are from several sources: sampling error, uncertainty in the diffusion coefficient, tracking error, vibration, and drift. Theoretical, computational, and experimental determinations of these sources of error show that the contribution of each is set by the method used to calculate the diffusion coefficient, Method 1 or Method 2. In Method 1, sampling error (and possibly the uncertainty in bead radius and temperature) will set the precision of the measurement, while tracking error and vibrational noise will cause an overestimate in the diffusion coefficient. In Method 2, both the precision and accuracy of the measured diffusion coefficient will be dominated by sampling error. When we reduce these sources of error (sampling error, tracking error, vibration, and drift) we are able to measure the diffusion coefficient to within 1% of the nominal value.

We hope this work will serve as a guide for faculty looking to improve the quantification of Brownian motion experiments, allowing students to focus on the science that convinced Otswald of the atomic nature of matter.

ACKNOWLEDGMENTS

The authors would like to thank Amy Wagaman for careful reading of the manuscript. This work was supported by a Howard Hughes Medical Investigator undergraduate fellowship (MAC), a SOMAS-URM grant (JGT), and Amherst College.

APPENDIX A: SYSTEMATIC UNCERTAINTY IN THE DIFFUSION COEFFICIENT

If the uncertainty in D is systematic, not random, then we will miscalculate the nominal value of D. Systematic errors in the bead radius can be estimated by finding the standard deviation of the mean bead radius, which depends on the

number of beads used to determine the value. Typical counts are on the order of ~500 beads (Invitrogen and Spherotech), indicating that the fractional standard error of the mean is 0.1% and can be ignored. Systematic errors in the temperature are much more problematic. For our experimental setup we measure the average temperature at the sample plane to be up to 1.2 °C higher than the average room temperature, due to heating by the illumination system. If room temperature is used, this would produce an underestimate in the nominal value of D by 3% and an overestimate in the Boltzmann constant by the same amount. Previously reported overestimates[12] in the Boltzmann constant may be due to this systematic error. Other systematic errors include a well-known overestimate in the diffusion coefficient when the bead is proximal to the sample surface or to another bead.[30] We use large sample chambers (300 μm thick) and dilute solutions (~10 μm between beads) so that the correction in the diffusion coefficient is <0.5%. Thus, while systematic errors in the nominal value should be taken into account, careful planning of the experiment by the faculty member can eliminate these systematic errors.

APPENDIX B: REDUCTION OF VIBRATIONAL NOISE

To use Method 1 to accurately measure the diffusion coefficient we need to reduce tracking error and vibrational noise. In our original data (Sec. II), the mechanical noise in the system is actually quite low. Figure 4(b) shows that the microscope drift is about 1 nm/s for the 800-s trace. The vibration as measured by the standard deviation for the trace is ~20 nm at 10 Hz. In addition, there is no fluid flow in the sample as the average bead displacement is zero [Fig. 1(e)]. According to our simulation, both drift and vibration at that level would be negligible. This was unexpected since the microscope is located on the second floor in a high-traffic area and does not have an active vibration-isolation system. However, the microscope used for the experiment does sit on a large cast iron table that passively reduces mechanical noise. For other faculty that are not as lucky, there are sophisticated "de-drifting" algorithms that measure the correlated noise between a series of beads in a frame and remove this correlated motion.[27,31] In this case, switching to MATLAB tracking software would be one way to computationally remove mechanical noise. In addition, similar passive systems can be purchased for a fraction of the cost of an active vibration-isolation system.

[a]Electronic mail: acarter@amherst.edu

[1]J. A. Earl and F. E. Christensen, "Brownian motion determination of Avogadro's number," Am. J. Phys. **33**(3), xxi–xxii (1965).
[2]Noel A. Clark, Joseph H. Lunacek, and George B. Benedek, "A study of Brownian motion using light scattering," Am. J. Phys. **38**(5), 575–585 (1970).
[3]George Barnes, "A Brownian motion demonstration using television," Am. J. Phys. **41**(2), 278–280 (1973).
[4]Robert Stoller, "Viewing Brownian motion with laser light," Am. J. Phys. **44**(2), 188 (1976).
[5]Haym Kruglak, "Boltzmann's constant: A laboratory experiment," Am. J. Phys. **57**(3), 216–217 (1989).
[6]Walter Connolly and Bill Reid, "Viewer for Brownian motion," Phys. Teach. **29**(1), 52–53 (1991).
[7]Se-yuen Mak, "Brownian motion using a laser pointer," Phys. Teach. **36**(6), 342–343 (1998).
[8]Paul Nakroshis, Matthew Amoroso, Jason Legere, and Christian Smith, "Measuring Boltzmann's constant using video microscopy of Brownian motion," Am. J. Phys. **71**(6), 568–573 (2003).
[9]Jeremy Bernstein, "Einstein and the existence of atoms," Am. J. Phys. **74**(10), 863–872 (2006).
[10]Ronald Newburgh, Joseph Peidle, and Wolfgang Rueckner, "Einstein, Perrin, and the reality of atoms: 1905 revisited," Am. J. Phys. **74**(6), 478–481 (2006).
[11]Dongdong Jia, Jonathan Hamilton, Lenu M. Zaman, and Anura Goonewardene, "The time, size, viscosity, and temperature dependence of the Brownian motion of polystyrene microspheres," Am. J. Phys. **75**(2), 111–115 (2007).
[12]J. Peidle, C. Stokes, R. Hart, M. Franklin, R. Newburgh, J. Pahk, W. Rueckner, and A. Samuel, "Inexpensive microscopy for introductory laboratory courses," Am. J. Phys. **77**(10), 931–938 (2009).
[13]P. Pearle, B. Collett, K. Bart, D. Bilderback, D. Newman, and S. Samuels, "What Brown saw and you can too," Am. J. Phys. **78**(12), 1278–1289 (2010).
[14]Robert Brown, "A brief account of microscopical observations made … on the particles contained in the pollen of plants; and on the general existence of active molecules in organic and inorganic bodies," Philos. Mag. **4**(21), 161–173 (1828).
[15]A. Einstein, *Investigations on the Theory of the Brownian Movement* (Dover Publications, Mineola, NY, 1956).
[16]J. Perrin and F. Soddy, *Brownian Movement and Molecular Reality* (Dover Publications, Mineola, NY, 2005).
[17]Nico Stuurman, MTRACK2, <http://valelab.ucsf.edu/~nico/IJplugins/MTrack2.html> (2009).
[18]T. M. Nordlund, *Quantitative Understanding of Biosystems: An Introduction to Biophysics* (Taylor & Francis, London, 2010).
[19]See supplementary material at http://dx.doi.org/10.1119/1.4803529 for a MATLAB program to simulate noise in Brownian Motion experiments and a program written in IGOR to visualize a two-dimensional random walk.
[20]J. R. Taylor, *An Introduction to Error Analysis: The Study of Uncertainties in Physical Measurements* (University Science Books, 1997).
[21]T. G. Mason, K. Ganesan, J. H. van Zanten, D. Wirtz, and S. C. Kuo, "Particle tracking microrheology of complex fluids," Phys. Rev. Lett. **79**(17), 3282–3285 (1997).
[22]U. C. Berkeley Advanced Lab, "Simulating Brownian motion," <http://www.advancedlab.org/mediawiki/index.php/Simulating_Brownian_Motion> (2011).
[23]J. Kestin, J. V. Sengers, B. Kamgar-Parsi, and J. M. H. Levelt Sengers, "Thermophysical properties of fluid H_2O," J. Phys. Chem. Ref. Data. **13**(1), 175–183 (1984).
[24]P. S. Mann, *Introductory Statistics* (John Wiley & Sons, Hoboken, NJ, 2010).
[25]H. Saka, R. D. Bengtson, and L. E. Reichl, "Relaxation of Brownian particles in a gravitational field," Am. J. Phys. **77**(3), 240–243 (2009).
[26]Ashley R. Carter, Gavin M. King, Theresa A. Ulrich, Wayne Halsey, David Alchenberger, and Thomas T. Perkins, "Stabilization of an optical microscope to 0.1 nm in three dimensions," Appl. Opt. **46**(3), 421–427 (2007).
[27]Vincent Pelletier, Naama Gal, Paul Fournier, and Maria L. Kilfoil, "Microrheology of microtubule solutions and actin-microtubule composite networks," Phys. Rev. Lett. **102**(18), 188303 (2009).
[28]Maria Kilfoil, "Biological physics software," <http://people.umass.edu/kilfoil/downloads.html> (2012).
[29]P. I. Good, *Resampling Methods: A Practical Guide to Data Analysis* (Birkhäuser, Boston, 2005).
[30]John C. Crocker, "Measurement of the hydrodynamic corrections to the Brownian motion of two colloidal spheres," J. Chem. Phys. **106**(7), 2837–2840 (1997).
[31]John C. Crocker and Brenton D. Hoffman, "Multiple particle tracking and twopoint microrheology in cells," Cell Mech. **83**, 141–178 (2007).
[32]Josef Trapani, "Brownian motion simulator," <http://www.igorexchange.com/project/BM_simulator> (2012).